AIAA 2014-1044

AIAA SciTech
13-17 January 2014, National Harbor, Maryland
55th AIAA/ASMe/ASCE/AHS/SC Structures, Structural Dynamics, and Materials Conference

Preliminary Assessment of Optimal Longitudinal-Mode Control for Drag Reduction through Distributed Aeroelastic Shaping

Corey Ippolito[1] and Nhan Nguyen[2]
NASA Ames Research Center, Moffett Field, CA 94035

Jason Lohn[3]
Carnegie Mellon University in Silicon Valley, Moffett Field, CA 94035

and

John Dolan[4]
Carnegie Mellon University, Pittsburgh, PA

The emergence of advanced lightweight materials is resulting in a new generation of lighter, flexible, more-efficient airframes that are enabling concepts for active aeroelastic wing-shape control to achieve greater flight efficiency and increased safety margins. These elastically shaped aircraft concepts require non-traditional methods for large-scale multi-objective flight control that simultaneously seek to gain aerodynamic efficiency in terms of drag reduction while performing traditional command-tracking tasks as part of a complete guidance and navigation solution. This paper presents results from a preliminary study of a notional multi-objective control law for an aeroelastic flexible-wing aircraft controlled through distributed continuous leading and trailing edge control surface actuators. This preliminary study develops and analyzes a multi-objective control law derived from optimal linear quadratic methods on a longitudinal vehicle dynamics model with coupled aeroelastic dynamics. The controller tracks commanded attack-angle while minimizing drag and controlling wing twist and bend. This paper presents an overview of the elastic aircraft concept, outlines the coupled vehicle model, presents the preliminary control law formulation and implementation, presents results from simulation, provides analysis, and concludes by identifying possible future areas for research.

I. Introduction

Continuing advances in modern engineered materials and the need for greater efficiency of aircraft in flight are driving new aircraft design concepts that incorporate lightweight flexible multi-functional structures. These new structural concepts provide less rigidity while maintaining the same load-carrying capacity as previous generation designs. The Boeing 787 Dreamliner aircraft's highly flexible wing structure is an example of this emerging trend. These advances are also driving research into active aeroelastic shape control of these flexible aircraft structures during flight. For instance, elastically shaping an aircraft by actively controlling wing wash-out twist and wing bending deflection in order to change the local angle of attack has the potential to yield lower fuel burn by drag reduction during cruise. Structural flexibility can further be leveraged to realize a revolutionary, optimal wing shape design that can accommodate a significant curvature for drag reduction benefits.

A conceptual study was recently conducted outlining the concept for Adaptive Aeroelastic Shape Control (AASC)[1]. This study outlines plans for multi-disciplinary design, analysis and optimization to examine the potential

[1] Research Scientist, Intelligent Systems Division, NASA Ames Research Center. AIAA Member
[2] Research Scientist, Intelligent Systems Division, NASA Ames Research Center. AIAA Associate Fellow
[3] Associate Research Professor, Carnegie Mellon University Silicon Valley, Moffett Field, CA
[4] Principal Systems Scientist, Robotics Institute, Carnegie Mellon University, Pittsburgh, PA

benefits of AASC on a flexible aircraft in flight over a conventional aircraft with traditional flight control system design.

Four major technical areas of AASC research were outlined in this study:

1. Vehicle concept design and optimization
2. Aeroelastic flight dynamic modeling
3. Elastically wing shaping actuation design
4. Flight control design and vehicle simulation

Significant research activity has occurred on the AASC in several of these areas, including a distributed actuation system for effecting elastic shape control [2], investigation of non-linear coupling between aeroelastic modes and the flight vehicle dynamics [3], development of a coupled high-fidelity numerical model utilizing vortex-lattice and finite-element methods [4], offline shape optimization studies for drag minimization [5,6], and development of a lower-order aeroelastic vehicle model that is appropriate for control law development [7].

This study builds on results from this previous research and focuses on flight control design in technical area 4 above. Research under this area seeks to develop multi-objective flight control to simultaneously gain aerodynamic efficiency while maintaining traditional pilot command-tracking tasks for guidance and navigation. Research in this area also seeks to develop guidance laws to achieve low drag objectives, with specific focus on the cruise segment of flight, applying modern multi-objective optimal control techniques for control of elastically-shaped aircraft.

This paper presents a preliminary study of a notional multi-objective control law for an elastically-shaped flexible-wing aircraft with distributed leading and trailing edge control surface actuators. The purpose of this initial study is to determine feasibility of a centralized control framework that simultaneously minimizes drag, stabilizes structural modes, and simultaneously performs longitudinal attack-angle command-tracking tasks. This initial study continues the previous research by implementing the proposed control concept [7], utilizing distributed control surface actuation for control of the coupled aeroelastic and flight dynamics model. This study develops a multi-objective control structure in a standard unconstrained linear-quadratic optimization framework and implements this controller on the recently developed model. The goals of this initial study are to demonstrate feasibility of this approach using a preliminary control concept, provide an assessment of expected performance improvements, identify challenges, and outline directions for future research to enable large-scale multi-objective control of aeroelastically shaped vehicles.

This paper is organized as follows. The concept for elastically-shaped aircraft is presented, followed by a coupled aeroelastic flight dynamics model on which this work is based. The optimal control problem is formalized, the solution is presented, and the simulation implementation is presented. The closed-loop response of the system is presented with a focus on estimating quantifiable performance benefits. The results will be discussed, limitations identified, and directions for future work presented.

II. Elastically Shaped Aircraft Model

The model[4] utilized in this study describes the longitudinal dynamics of a generic transport aircraft at Mach 0.80 and Mach 0.88 at an altitude of 35,000 ft. The longitudinal dynamics are described by two aircraft states: angle of attack α and pitch rate q. The aircraft model contains 80 structural states capturing the 20 dominant flexible modes, and provides 23 control inputs: one elevator, 11 flaps, and 11 slats; as shown in Figure 1.

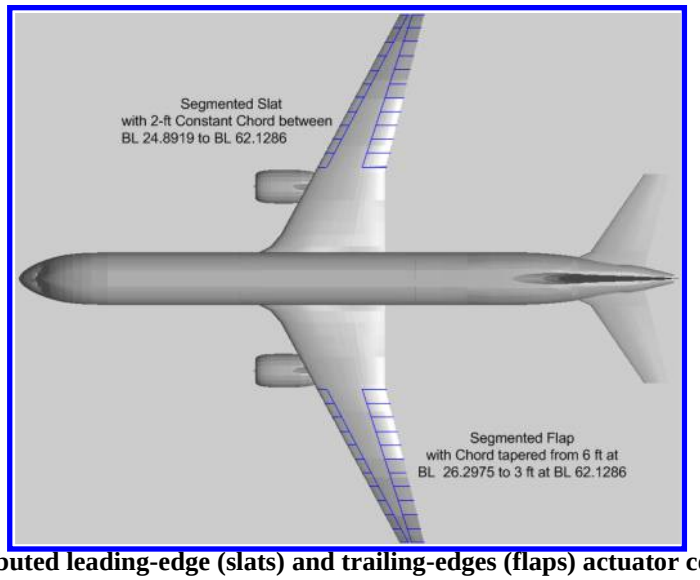

Figure 1. Distributed leading-edge (slats) and trailing-edges (flaps) actuator configuration.

The coupled equations of motion are given by

$$\begin{bmatrix}\dot{x}_r\\ \dot{x}_e\end{bmatrix} = \begin{bmatrix}A_{rr} & A_{re}\\ A_{er} & A_{ee}\end{bmatrix}\begin{bmatrix}x_r\\ x_e\end{bmatrix} + \begin{bmatrix}B_{rr} & B_{re}\\ B_{er} & B_{ee}\end{bmatrix}\begin{bmatrix}u_r\\ u_e\end{bmatrix} \tag{1}$$

where the states are given by $x_r = [\alpha \quad q]^T$, $x_e = [q_w \quad q_\theta \quad \dot{q}_w \quad \dot{q}_\theta]^T$, and $q_w, q_\theta \in \mathbb{R}^m$ are the generalized coordinate vectors for bending and torsion, respectively, along with their derivatives $\dot{q}_w, \dot{q}_\theta \in \mathbb{R}^m$. The elements of q_w and q_θ are indexed such that q_{w_i} and q_{θ_i} are the wing bending and torsional deflections of mode i = 1,…,m, where m=20 is the total number of mode shapes. The input $u_r = [\delta_e]$ is the elevator flap deflection angle, and $u_e = [\delta_f \quad \delta_s]^T$ where δ_f is the vector of 11 distributed flap inputs and δ_s is the vector of 11 distributed slat inputs. This results in a model with 82 states and 23 inputs. This initial study assumes all aeroelastic modes and vehicle states are observable.

The lift and drag characteristics of the aircraft are functions of the current vehicle states, flexible-mode states, and control inputs as described by the following equations

$$C_D = C_{D_0} + K\left(C_{L_0} + C_{L_x}x + C_{L_u}u\right)^2 + C_{D_u}u + u^T C_{D_{u^2}}u \tag{2}$$

where K is the drag polar parameter, C_D is the total drag coefficient, and C_L is the total lift coefficient.

III. Control Law Formulation

The control system is designed using full-state feedback with attack-angle tracking-error integrator feedback as developed in the literature [4] and summarized here. This formulation extends the model to include pitch-rate tracking as well as a reference signal filter. The controller tracks a commanded angle of attack signal, α_c. Two integrator states α_I, q_I integrate the reference error signals for control, given by

$$\begin{aligned}\dot{\alpha}_I &= \alpha_r - \alpha\\ \dot{q}_I &= q_r - q\end{aligned} \tag{3}$$

The reference model filter combined with the integrators above can be expressed as

$$\dot{x}_c = A_{cc}x_c + A_{cr}x_r + B_{cz}z$$
$$A_{cc} = \begin{bmatrix}0 & 0 & 1 & 0\\ 0 & 0 & 0 & 1\\ 0 & 0 & 0 & 1\\ 0 & 0 & -\omega_r^2 & -2\omega_r\end{bmatrix} \;;\; A_{cr} = \begin{bmatrix}-1 & 0\\ 0 & -1\\ 0 & 0\\ 0 & 0\end{bmatrix} \;;\; B_{cz} = \begin{bmatrix}0\\ 0\\ 0\\ \omega_r^2\end{bmatrix} \tag{4}$$

where $x_c = [\alpha_I \; q_I \; \alpha_r \; q_r]'$ and $z = [\alpha_c]$ is the input reference signal. The reference model in (4) is appropriate for the model given in (1) which has two states, α and q. Combining the systems in (4) and (1) forms the augmented system, given by

$$\dot{x} = Ax + Bu + B_z z$$
$$y = Cx + Du \tag{5}$$

where $x \in \mathbb{R}^N$ is of size N=86 and $u \in \mathbb{R}^M$ is of size M=23, and

$$x = [x_r\ x_e\ x_a]^T\ ;\ u = [u_r\ \ u_e]^T\ \ ;\ \ z = [\alpha_{cmd}]$$
$$A = \begin{bmatrix} A_{rr} & A_{re} & 0 \\ A_{er} & A_{ee} & 0 \\ A_{cr} & 0 & A_{cc} \end{bmatrix};\ B = \begin{bmatrix} B_{rr} & B_{re} \\ B_{er} & B_{ee} \\ 0 & 0 \end{bmatrix};\ B_z = \begin{bmatrix} 0 \\ 0 \\ B_{cz} \end{bmatrix}\ ;\ C = I\ ;\ D = 0 \tag{6}$$

The optimal control formulation utilizes a cost function J with quadratic costs terms to address the multiple control objectives.

$$J(x,u,t) = \frac{1}{2}\int_0^\infty (x^T Q x + u^T R u + q_d C_D) dt \tag{7}$$

The weighting matrix $Q = diag\{Q_r, Q_e, Q_c\}$ and its submatrices are diagonal matrices which regulate vehicle states x_r, aeroelastic states x_e, and the control reference model x_c, respectively. Similarly, $R = diag\{R_f, R_s, R_e\}$ and its submatrices penalize control actuation effort of the flaps, slats, and elevator, respectively. The drag coefficient C_D term is included in the cost function with weight q_d. Substituting in J yields

$$J(x,u,t) = \frac{1}{2}\int_0^\infty \Big(x^T Q x + u^T R u + q_d C_{D_0} + q_d K\big(C_{L_0} + C_{L_x} x + C_{L_u} u\big)^2 + q_d C_{D_u} u + u^T q_D C_{D_{u^2}} u\Big)\, dt \tag{8}$$

The Hamiltonian equation is given by

$$H = \frac{1}{2}\Big[x^T Q x + u^T R u + q_d C_{D_0} + q_d K\big(C_{L_0} + C_{L_x} x + C_{L_u} u\big)^2 + q_d C_{D_u} u + u^T q_d C_{D_{u^2}} u\Big] + \lambda^T (Ax + Bu + B_z z) \tag{9}$$

The control solution for problems of this form[7] is given by

$$u(x,z) = u_x x + u_z z + u_c \tag{10}$$

where

$$u_x = -\bar{R}^{-1}\big(B^T P + q_d K C_{L_u}^T C_{L_x}\big)$$
$$u_z = -(\bar{R}^{-1} B^T S)$$
$$u_c = -\bar{R}^{-1}\left(q_d K C_{L_u}^T C_{L_0} + \frac{1}{2} q_d C_{D_u}^T + B^T \lambda_0\right) \tag{11}$$

The value of P is found from the solution to the following algebraic Riccati equation

$$P\bar{A} + \bar{A}^T P - PB\bar{R}^{-1}B^T P + \bar{Q} = 0 \tag{12}$$

where

$$\bar{R} = R + q_d K C_{L_u}^T C_{L_u} + q_d C_{D_{u^2}}$$
$$\bar{A} = A - B\bar{R}^{-1} q_d K C_{L_u}^T C_{L_x}$$
$$\bar{Q} = Q + q_d K C_{L_x}^T \big(C_{L_x} - C_{L_u}\bar{R}^{-1} q_d K C_{L_u}^T C_{L_x}\big) \tag{13}$$

and

$$S = (PB\bar{R}^{-1}B^T - \bar{A}^T)^{-1} P B_z$$
$$\lambda_0 = (PB\bar{R}^{-1}B^T - \bar{A}^T)^{-1}\Big(q_d K C_{L_x}^T C_{L_0} - \big(PB + q_d K C_{L_x}^T C_{L_u}\big)\bar{R}^{-1}\left(q_d K C_{L_u}^T C_{L_0} + \frac{1}{2} q_d C_{D_u}^T\right)\Big) \tag{14}$$

The sufficient condition for a solution to exist requires checking the following, from which $\bar{Q} > 0$ can be inferred[7].

$$q_d K C_{L_u}^T C_{L_x} < \bar{R} \tag{15}$$

IV. Implementation

Forming the closed loop system of (5) under the feedback law (10) yields

$$\dot{x} = (A + Bu_x)x + (Bu_z + B_z)z + Bu_c \tag{16}$$

Note that the u_c term is constant in the derivative equation in (16), resulting in component x_s of the state vector given by

$$\begin{gathered} \tilde{x} = x + x_s \\ x_s = A^{-1}B\bar{R}^{-1}\left(q_d K C_{L_u}^T C_{L_0} + \frac{1}{2} q_d C_{D_u}^T + B^T \lambda_0\right) \end{gathered} \tag{17}$$

where $\tilde{x}$ is the complete solution state vector. Equation (17) must be solved using the original system matrix $\begin{bmatrix} A_{rr} & A_{re} \\ A_{er} & A_{ee} \end{bmatrix}$, which is invertible, and the effect of the constant u_c term in the integrator can be solved separately.

For evaluation of drag reduction, we define an average drag metric which integrates ΔC_D over the specified time interval.

$$C_{D_{avg}} = \frac{1}{t_f}\int_0^{t_f} \Delta C_D dt \tag{18}$$

The state and aeroelastic weighting matrices were initially selected based on Bryson's criteria, which set the initial weighting elements based on the maximum expected value of the state and input elements. The Q and R diagonal matrices are given by

$$\begin{gathered} Q_r = k_{Qr} \cdot diag\left[\frac{1}{\alpha_{max}^2}, \frac{1}{q_{max}^2}\right] \\ Q_e = k_{Qe} \cdot diag\left[1/q_{w_{max}}^2 \quad 1/q_{\theta_{max}}^2 \quad 1/\dot{q}_{w_{max}}^2 \quad 1/\dot{q}_{\theta_{max}}^2\right] \\ Q_c = k_{Qc} \\ R_r = k_{re} \cdot \left[\frac{1}{\delta_{e_{max}}^2}\right] \\ R_e = diag\left\{k_{rf} \cdot diag\left[\frac{1}{maxexp\left(u_{e_i}\right)^2}\right], k_{rs} \cdot diag\left[\frac{1}{maxexp\left(u_{e_i}\right)^2}\right]\right\} \end{gathered} \tag{19}$$

The scalar parameter set $k = \{q_d, k_{Qr}, k_{Qe}, k_{Qa}, k_{Re}, k_{Rs}, k_{Rf}\}$ allows for tuning of relative weights in the cost function as permissible, subject to the conditions in (15).

The controller was implemented in a MATLAB Simulink simulation environment utilizing the model given in (5). The Simulink model is summarized in Figure 2.

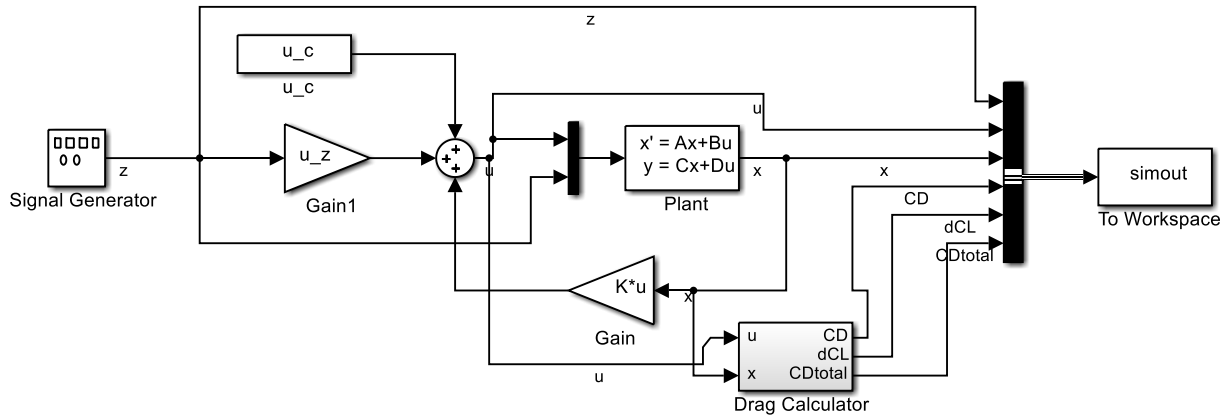

Figure 2. Matlab Simulink Model

V. Simulation Results

Evaluation of the open loop models for both Mach 0.80 and Mach 0.88 shows that the two models are similar in structure and have unstable open-loop modes. Both models are controllable and the unstable modes can be stabilized through LQR feedback, as illustrated in Figure 3.

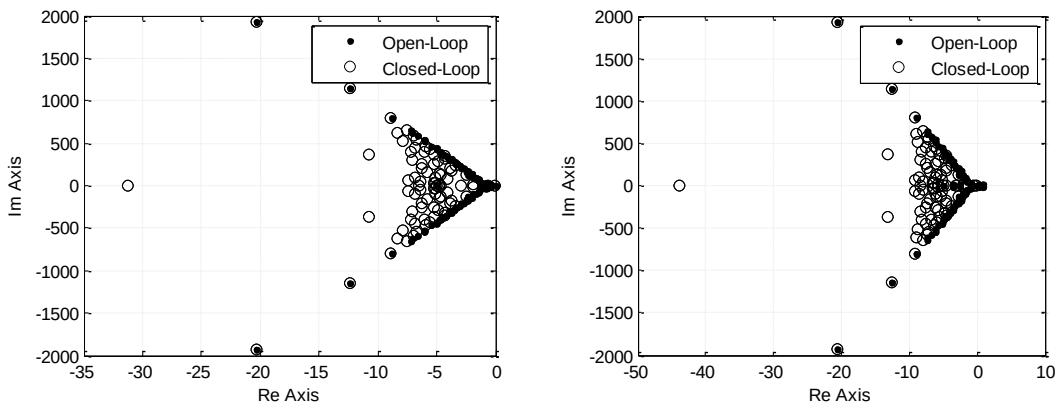

Figure 3. Open-loop and closed-loop poles. *Shown for Mach 0.80 model (left) and Mach 0.88 model (right). The M0.80 has no unstable poles, the M0.88 model has 4 unstable poles which are stabilized in feedback.*

Tracking performance was first evaluated by setting integrators Q weights high ($k_{Q_c,1} = k_{Q_c,2}$=1e4), other Q weights low (k_{Q_i}=1e-5), and R weights $k_R = 0.1$ to prevent excessive actuation. The response of the system to an initial offset with zero input is shown below.

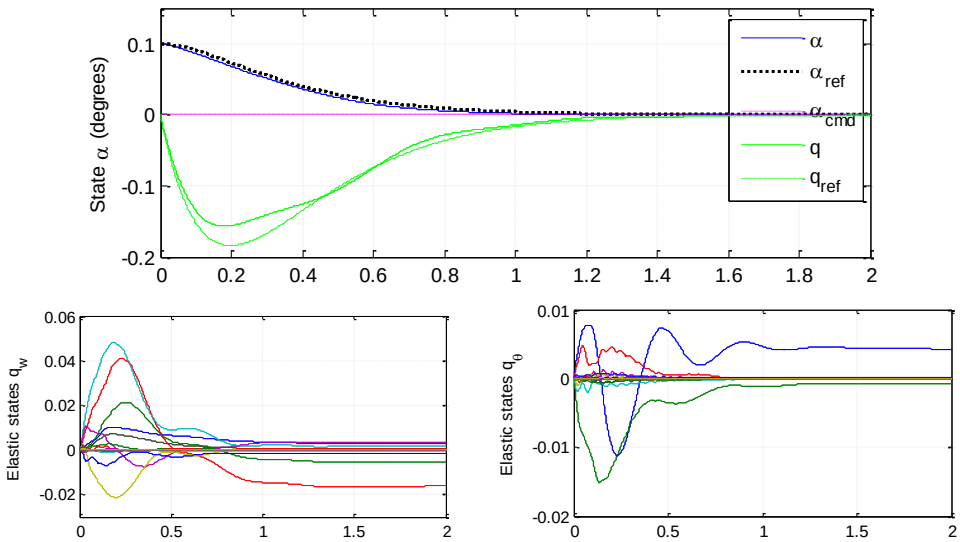

Figure 4. Response to initial offset with zero command signal. *Shown with reference model filter $\omega_r = 5$. Aircraft tracking signals q and α are shown to their reference signals.*

The command filter frequency ω_r shapes the reference signal response curve based on desired aircraft response, as shown in Figure 5 below in response to doublet inputs. Note that aggressive filter selection results in larger drag spikes due to larger maneuvering control surface loads, but the controller tracks well under aggressive performance demands. A frequency of ω_r=5.0 was used as the reference filter response rate in this report.

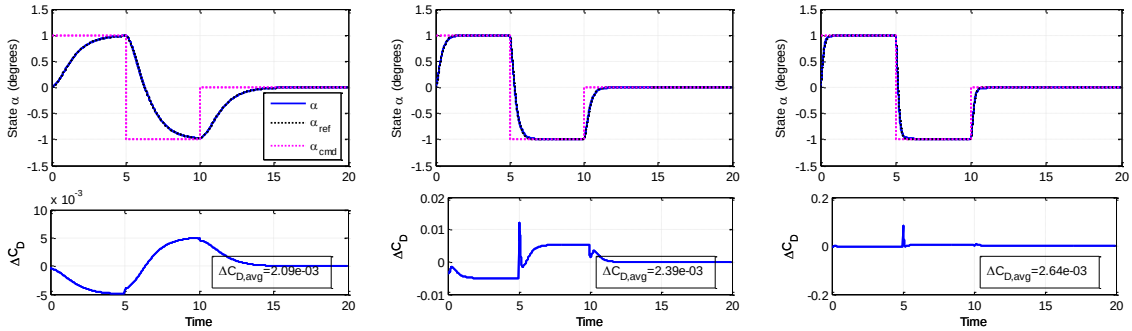

Figure 5. Attack angle tracking varying with command reference filter. *Attack angle (top) shown for varying reference filter frequencies (from left to right) ω_r={1.3, 5.0, 10}. Resulting ΔCD is shown in the lower graphs.*

The system response at the selected frequency is shown in Figure 6. The α and q tracking plots (top two graphs on the left column in Figure 6) show tracking of the reference model and vehicle states from α square-wave commands. The control surface responses (top two graphs on right column) show summary of the distributed control surface deflections. The drag response (bottom left graph) shows a positive drag correlation to attack-angle, with increased drag occurring during maneuvers to achieve the commanded q rates. The bottom right graph shows how the control surface deflections occur for the flaps and slats at steady state (t=3.3) and at the time of their maximum deflection.

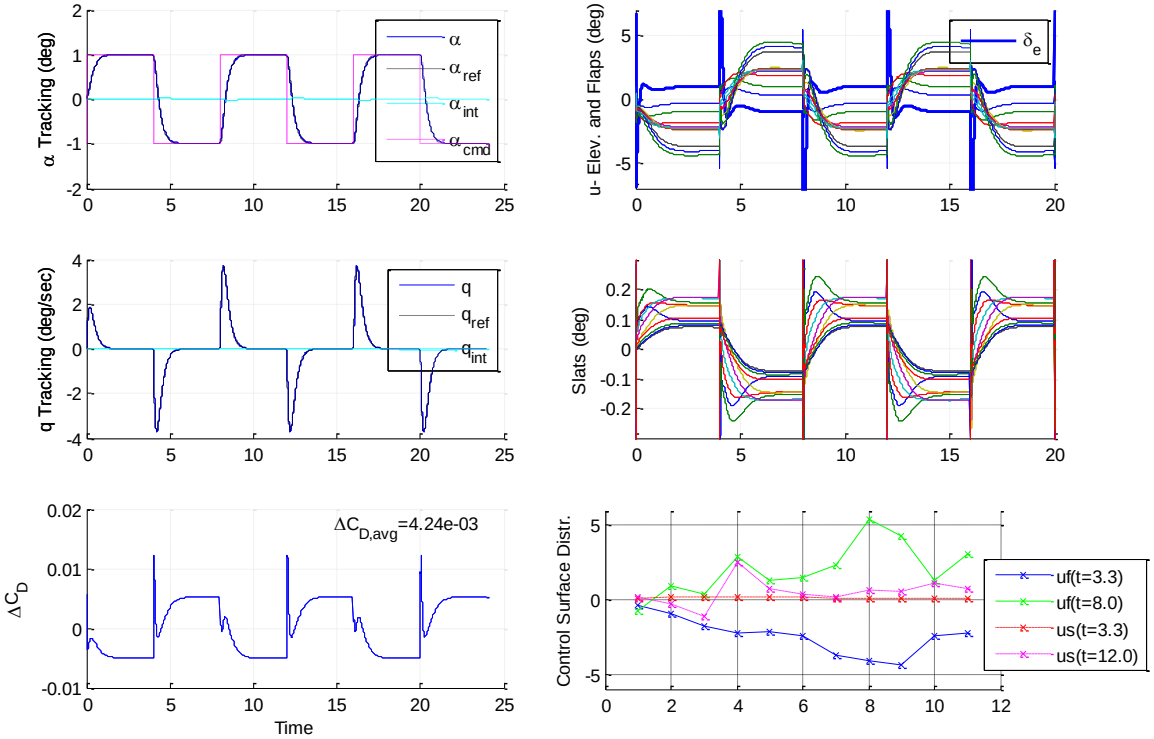

Figure 6. Baseline controller, square-wave input response.

Adjusting Q and R matrix gains to include drag reduction objectives, it was found that q_d=1e2, $k_{Qc,1} = k_{Qc,2}$=1e2, k_{Qe}=1e-2, k_R= 1.0, and $k_{Qc,3} = k_{Qc,4} = k_{Qr}$=1e-10 maintains good tracking of the command signal while providing a reduction in drag.

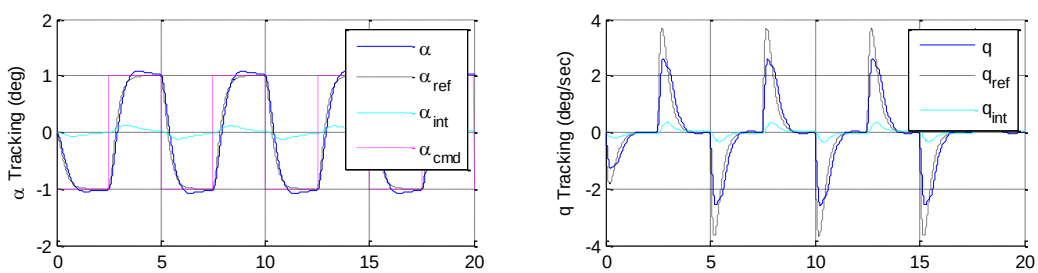

Figure 7. Tracking Results. *Shown with q_d=$k_{Q,C1} = k_{Q,C2}$=1e2, k_{Qe}=1e-2, k_R= 1.0, and $k_{Qc,3} = k_{Qc,4} = k_{Qr}$=1e-10.*

The aeroelastic bending and torsion modes for this configuration are shown below in comparison to the resulting flap and slat deflections.

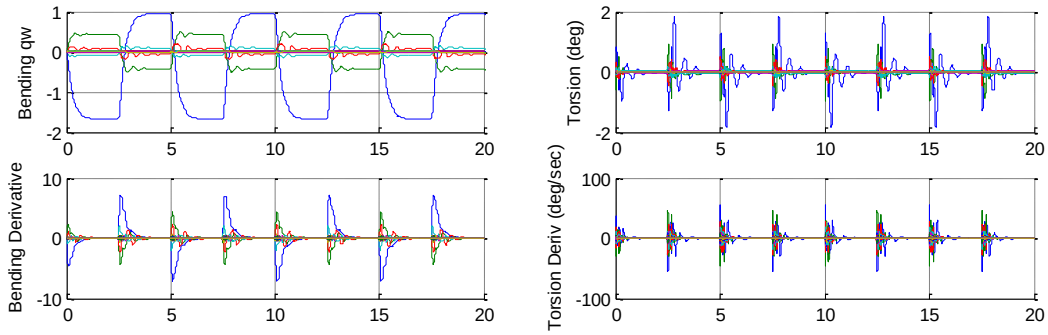

Figure 8. Aeroelastic Bending and Torsion States. *Shown with* k_d=$k_{Q,C1}$ = $k_{Q,C2}$=*1e2,* k_{Qe}=*1e-2,* k_R= *1.0, and* $k_{Q,C3}$ = $k_{Q,C4}$ = $k_{Q,C3}$ = $k_{Q,R}$=*1e-10.*

The resulting wing shape and control surface deflections are shown below at two times: when the first input stabilizes, and at the time of maximum flap and slat deflection.

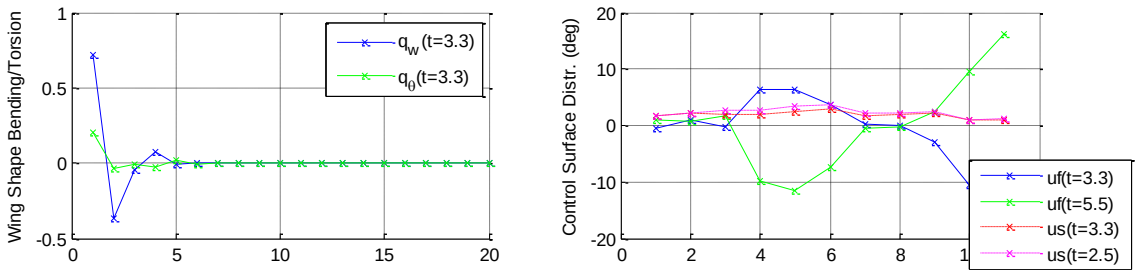

Figure 9. Wing shape and Control Surface

The baseline control provides the drag profile shown below, which results in an overall drag increase of $\Delta C_{D,Total}$=1.72e-03 during the maneuver.

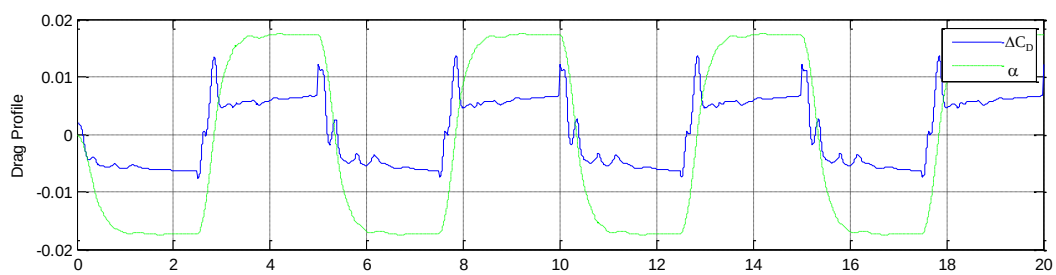

Figure 10. Delta Drag Profile for Baseline State-Tracking Controller.

The resulting drag profile for the Mach 0.80 model is shown below, which results in an overall decrease in drag of $\Delta C_{D,Total}$=-1.69e-03 during the maneuver.

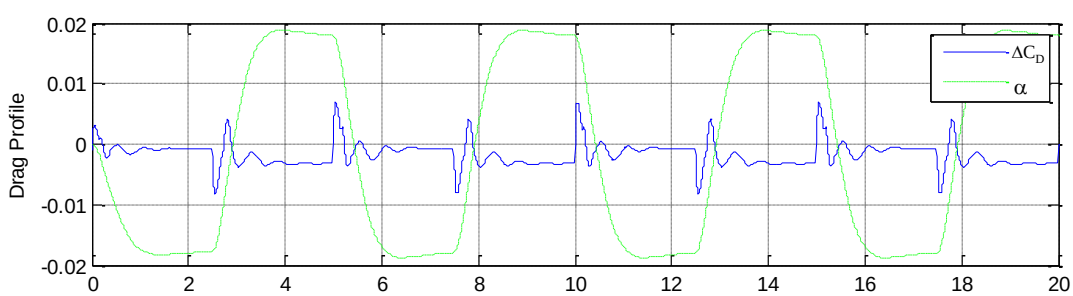

Figure 11. Delta Drag Profile. *Shown for controller with drag reduction and state tracking objectives.*

The resulting drag for the two models compared between various controller settings is summarized in Table 1. The controller settings emphasize balanced gains, state control, and balanced drag reduction with state control.

Table 1. Controller Delta Drag Comparison.

Model	ΔCDavg	kd	kqr	kqe	kqc1	kqc2	kqc3	kqc4	kre	krs	krf
M0.80	1.72E-03	1	1	1	1	1	1	1	1	1	1
M0.80	6.61E-04	1E-5	1E-5	1E-5	1E+4	1E+4	1E-5	1E-5	1E-1	1E-1	1E-1
M0.80	-1.69E-03	1E+2	1E-10	1E-2	1E+2	1E+2	1E-10	1E-10	1	1	1
M0.88	1.71E-03	1	1	1	1	1	1	1	1	1	1
M0.88	4.84E-04	1E-5	1E-5	1E-5	1E+4	1E+4	1E-5	1E-5	1E-1	1E-1	1E-1
M0.88	-5.34E-03	1E+3	1E-10	2E-1	1E+2	1E+2	1E-10	1E-10	1	1	1

VI. Conclusion

The results of this study suggest that multiobjective AASC on an aeroelastic commercial transport aircraft can reduce overall drag for the aircraft in the cruise segment of flight while simultaneously performing standard flight control functions, such as responding to disturbances and performing maneuvers. This preliminary study has demonstrated feasibility of multi-objective drag-minimizing control for a flexible-wing aircraft with distributed actuators through a linear-quadratic control optimization framework. It has presented an initial implementation and refinement of a multiobjective control concept and has implemented the controller on a recently-derived aeroelastic vehicle model. The assessment presented, while of limited-scope, has produced an assessment of expected performance improvements. The multi-objective controller provides overall drag reduction on total aircraft and a reduction in drag as compared to the baseline single-objective controller. The controller was relatively straightforward to derive and the solution was readily computationally-solvable. Incorporation of high-level control gains in the control structure allowed intuitive adjustments to be made to the closed-loop system response. Inclusion of the integrator structure was likewise easy to accomplish, and suggests further structural modifications to the controller will not be problematic.

The results highlighted issues that will need to be addressed in further iterations of the control structure. In the preliminary control structure presented, the controller objective gains could be specified that resulted in unrealistically large control surface deflections. Control surfaces were unconstrained, ignoring relative deflection constraints between actuators and response speed constraints. The gains for tuning controller response provide a coarse mechanism to limit actuator response within a desired range. However, the control formulation can be derived as a constrained control problem to formally address these issues. The initial formulation included attack angle tracking only, but integrator overshoot and wind-up issues were observed in the response of this preliminary control structure. These were corrected through the addition of the model reference filter and the addition of q-rate tracking to produce an achievable and smoothly varying α_c based on the plant dynamics. The aircraft model used in this study is linearized; the effect of non-linear uncertainty may be of importance to consider. Direct sensing of all aeroelastic states will not likely be possible, and observer design will be incorporated into further iterations of this controller. Drag optimization in this study was based on an idealized drag polar, and methods for directly estimating and controlling drag may be necessary for achieving minimal drag on higher-fidelity models. Future research will investigate integration into a larger control design framework, including extending control to handle speed and lateral modes, and integration with outer-loop control structures or guidance trajectories signals. Multi-objective trajectory optimization can be utilized to provide additional drag-minimizing benefits, and trajectory-based control strategies[8] may be utilized to help improve tracking performance. Incorporating the wing-shape control targets found from offline optimization studies on the higher-fidelity numerical AASC model[5] should provide additional drag benefits. Finally, these controller and guidance and navigation solutions will be implemented and tested against the high-fidelity models and simulators that are currently in development.

Acknowledgments

The authors would like to thank the NASA Aeronautics Research Mission Directorate (ARMD) Fixed Wing Project under the Fundamental Aeronautics Program for providing support for this work. The authors would also like

to thank the members of the AASC project team and the Advanced Control and Evolvable Systems group at NASA Ames Research Center for their camaraderie, advice, and input in this research.

References

[1] Nguyen, N. "NASA Innovation Fund 2010 Project: Elastically Shaped Future Air Vehicle Concept," NASA Internal Report

[2] Urnes, J., Nguyen, N., Ippolito, C., Totah, J., Trinh, K., and Ting, E. "A Mission Adaptive Variable Camber Flap Control System to Optimize High Lift and Cruise Lift to Drag Ratios of Future N+3 Transport Aircraft" 51st AIAA Aerospace Sciences Meeting, Grapevine, TX, January 2013

[3] Nguyen, N., Trinh, K., Nguyen, D., Tuzcu, I., "Nonlinear Aeroelasticity of Flexible Wing Structure Coupled with Aircraft Flight Dynamics," AIAA Structures, Structural Dynamics, and Materials Conference, AIAA-2012-1792, April 2012.

[4] Nhan T. Nguyen, Eric B. Ting, Daniel Nguyen, Tung Dao, and Khanh T. "Coupled Vortex-Lattice Flight Dynamic Model with Aeroelastic Finite-Element Model of Flexible Wing Transport Aircraft with Variable Camber Continuous Trailing Edge Flap for Drag Reduction", AIAA Atmospheric Flight Mechanics (AFM) Conference. August 2013

[5] Ippolito, C., Nguyen, N., Totah, J., Trinh, K., Ting, E. "Initial Assessment of a Variable-Camber Continuous Trailing-Edge Flap System on a Rigid Wing for Drag Reduction in Subsonic Cruise" AIAA Infotech@Aerospace (I@A) Conference, August 19-22, 2013, Boston, MA

[6] Nguyen, N., Trinh, K., Reynolds, K., Kless, J., Aftosmis, M., Urnes, J. "Elastically Shaped Wing Optimization and Aircraft Concept for Improved Cruise Efficiency" AIAA Paper 2013, Vol 141, 2013

[7] Nguyen, N., Urnes, J. "Aeroelastic Modeling of Elastically Shaped Aircraft Concept via Wing Shaping Control for Drag Reduction". AIAA Atmospheric Flight Mechanics Conference. 13 - 16 August 2012, Minneapolis, Minnesota

[8] Adami, T., Zhu, J., Ishihara, A., Yeh, Y., Ippolito, C. "Six-DOF trajectory tracking for payload directed flight using trajectory linearization control". Proc. of AIAA Guidance, Navigation and Control Conference, Seattle, Washington. Pg 1897-1916. 2009